

Article

Not peer-reviewed version

Low Frequency Raman Spectroscopy on Amorphous Poly(Ether Ether Ketone) (PEEK)

Tomoko Numata , Naomoto Ishikawa , [Toshihiro Shimada](#) , [Keith C Gordon](#) , [Makoto Yamaguchi](#) *

Posted Date: 13 June 2024

doi: 10.20944/preprints202406.0875.v1

Keywords: Raman spectroscopy; thermoplastic polymer; PEEK; CFRP; crystallinity; amorphous



Preprints.org is a free multidiscipline platform providing preprint service that is dedicated to making early versions of research outputs permanently available and citable. Preprints posted at Preprints.org appear in Web of Science, Crossref, Google Scholar, Scilit, Europe PMC.

Copyright: This is an open access article distributed under the Creative Commons Attribution License which permits unrestricted use, distribution, and reproduction in any medium, provided the original work is properly cited.

Article

Low Frequency Raman Spectroscopy on Amorphous Poly(Ether Ether Ketone) (PEEK)

Tomoko Numata ^{1,2}, Naomoto Ishikawa ³, Toshihiro Shimada ⁴, Keith C. Gordon ⁵ and Makoto Yamaguchi ^{1,*}

¹ Department of Systems Design Engineering, Akita University, 1-1 Tegatagakuen-machi, Akita 010-8502, Japan

² Horiba Techno Service Co, Ltd., Chiyoda-ku, Tokyo, 101-0063, Japan

³ Kiguchi Technics inc., 114-15 Enoshima-cho, Yasugi-shi, 692-0057, Japan

⁴ Division of Applied Chemistry, Faculty of Engineering, Hokkaido University, Kita 13 Nishi 8, Kita-ku, Sapporo, 060-8628, Japan

⁵ Department of Chemistry, University of Otago, Dunedin, 9016, New Zealand

* Correspondence: yamaguci@gipc.akita-u.ac.jp; Tel.:+81-10-889-2344

Abstract: Low-frequency peaks in the Raman spectra of amorphous poly (ether ketone) (PEEK) are investigated. An amorphous sample with zero crystallinity, as confirmed by WAXRD, was used in this study. In a previous study, two peaks were observed in the low-frequency Raman spectra of crystallized samples. One of the peaks at 135 cm⁻¹, disappeared for the amorphous sample. Furthermore, the peak at 50 cm⁻¹ was observed for the first time in the crystallized sample. The peak at 50 cm⁻¹, similar to the peak at 135 cm⁻¹, disappeared in the amorphous state, and its intensity increased with increasing crystallinity. The origins of the two peaks were both associated with the Ph-CO-Ph-type intermolecular vibrational modes in the simulation. It was suggested that the Ph-CO-Ph vibrational mode observed in the low-frequency region of PEEK was strongly influenced by the intermolecular order.

Keywords: Raman spectroscopy; thermoplastic polymer; PEEK; CFRP; crystallinity; amorphous

1. Introduction

In recent years, carbon fiber-reinforced plastic (CFRP) has attracted attention in various fields, including aircraft and automobile fuselage materials, as an alternative to conventional steel materials because of their equivalent or superior strength and significant weight reduction. There are two primary types of CFRP: thermosetting CFRP, which uses a thermosetting polymer as the base material, and thermoplastic CFRP, which uses a thermoplastic polymer. Owing to the properties of thermoplastic polymers, which soften and melt when heated and solidify when cooled, thermoplastic CFRP has attracted attention in many fields because it requires a short molding time, is inexpensive, and has a high productivity [1]. Poly(ether ether ketone) (PEEK) is a high-performance thermoplastic polymer developed by Imperial Chemical Industries (now Victrex) in the UK that has excellent mechanical and chemical properties and thermal stability[2]. The degree of crystallinity of crystalline polymers greatly influences their mechanical, optical, electrical, and other practically important properties [3–7]. Evaluating the crystallinity of PEEK is one of the very important [8,9].

Various methods have been applied to evaluate the crystallinity of polymers including PEEK [9]. Wide-angle X-ray diffraction (WAXRD), differential scanning calorimetry (DSC)[10], and Fourier-transform infrared spectroscopy (FTIR)[8] are commonly used methods. In composite materials, it has been reported that the crystal structure of polymers and the behavior of crystal nucleus precipitation differ near fibers [11,12]. It is expected that the degree of crystallinity is spatially unevenly distributed owing to the influence of carbon fibers. Therefore, a crystallinity evaluation method with a high spatial resolution is required.

Raman spectroscopy is one of the most common techniques used to investigate polymer material [13]. It is also possible to obtain high spatial resolution using a microscopic optical system. Previous studies used Raman spectroscopy to assess the crystallinity of PEEK. [9,14–17]. On the other hand, as is well known, carbon materials have strong D- and G-band signals around 1600 cm^{-1} [18]. In composite materials, interference between the signals from carbon and polymer is a problem. Consequently, it is essential to employ frequencies within the range in which the carbon signal is absent. To solve this problem, we recently reported that the crystallinity of poly(ether ether ketone) (PEEK) can be evaluated using the peak in the low-frequency region ($<100\text{ cm}^{-1}$). [19]

Raman scattering in the low-frequency region is attracting attention in various fields because it has become easier to measure owing to the development of optical components. Similarly, research has been conducted in conjunction with THz spectroscopy, which has made remarkable progress in recent years. It has been reported that in some polymer materials, the peaks in low-frequency Raman scattering spectroscopy [20–23] and THz vibrational spectroscopy [24–26] are caused by intermolecular vibrations. Classical molecular dynamics (MD) simulations have shown that the vibrational mode in the terahertz region is an intermolecular vibrational mode for *n*-poly-L-lactide (PLLA). [27] In PEEK, it has been reported that intermolecular ordering affects low-frequency Raman spectra using MD simulations [28]; however, no direct experimental evidence has been reported. We investigated the behavior of low-frequency Raman spectra in an amorphous sample, which is thought to have no intermolecular order.

To use low-frequency peaks as reliable indicators of crystallinity, it is important to clarify their origins. The purpose of this study was to evaluate the Raman spectra of amorphous PEEK in the low-frequency region using a sample with zero crystallinity and to discuss the origin of these peaks.

2. Materials and Methods

2.1. Sample Preparation

A Grade 2000 APTIV PEEK film produced by Victrex ($t = 25\text{ }\mu\text{m}$), which is an unfilled amorphous film reported to have zero crystallinity [9], was used as the sample. Various degrees of crystallinity were achieved by heat-treating the as-received films. Samples with various degrees of crystallinity were obtained by heat-treating the as-received films. Heat treatment temperatures of $150\text{ }^{\circ}\text{C}$, $175\text{ }^{\circ}\text{C}$, $200\text{ }^{\circ}\text{C}$, $250\text{ }^{\circ}\text{C}$, and $300\text{ }^{\circ}\text{C}$ were chosen. The samples were maintained at the annealing temperature for 2 h in air before being cooled to room temperature in the same environment.

2.2. Experiments

WAXRD (Rigaku Ultima IV equipment) was employed at room temperature to determine crystallinity. $\text{CuK}\alpha$ X-rays with a wavelength of 0.154 nm were used, with a rotating anode operating at 40 kV and 30 mA . The diffraction angle, 2θ , ranged from 5° to 40° .

A micro-Raman spectroscopic system (Horiba HORIBA Jobin Yvon, LabRAM HR spectrometer) with a backscattering geometry was used. Using a $50\times$ objective lens, the spot diameter was approximately $1\text{ }\mu\text{m}$. In our PEEK sample, very strong fluorescence was observed when excited at 633 or 532 nm , which are the commonly used wavelengths in Raman scattering spectroscopy. To avoid fluorescence, infrared light with a wavelength of 1064 nm was selected as the excitation light. An InGaAs detector with $1.83\text{ cm}^{-1}/\text{pixel}$ resolution cooled liquid nitrogen was accumulated. The laser power incident on the sample was limited to 60 mW to avoid damage and further crystallization. The exposure time was 10 s and the number of integrations was four.

2.3. DFT and MD Simulation

Molecular vibrations of single-strand PEEK oligomers were calculated using density functional theory (DFT)(B3LYP/6-31G) in Gaussian16. The vibration of crystalline PEEK was calculated using molecular (MD) dynamics simulations in LAMMPS with generalized AMBER FF (GAFF). See references [29] for details of the calculations.

3. Results and Discussion

3.1. WAXRD Diffraction

Figure 1 shows the WAXRD diffractograms measured from 5 to 40° for each annealing temperature. Diffractograms are shown on the same scale and vertically shifted to show them clearly. Sharp peaks are observed at 2θ values of approximately 19°, 21°, 23°, and 29°, associated with the 110, 111, 200, and 211 planes, respectively [29]. The broad peak observed at approximately 19° was associated with the amorphous structure. Note that, in the as-received sample without annealing treatment, no crystallinity peak was observed, as in previous studies [9,30]. The crystallinity was determined by fitting each obtained WAXRD spectrum to separate sharp peaks due to crystallinity and broad peaks due to the amorphous structure of Lorentzian and Gaussian functions, respectively.

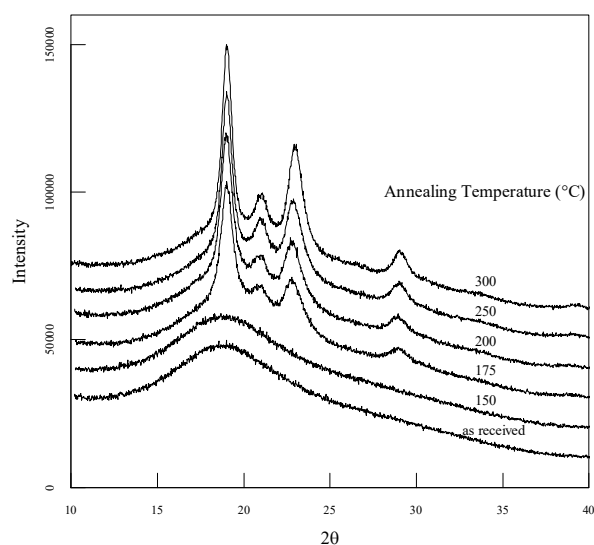


Figure 1. The WAXRD diffractograms were measured from 5° to 40° for each annealing temperature.

3.2. Raman Spectra

The Raman spectra of PEEK, standardized in the range of 40 cm^{-1} to 2000 cm^{-1} are shown in Fig. 2. For clarity, they are shown to be shifted vertically. Several strong peaks were observed in the low- and mid-frequency regions of all the spectra. The origins of the peaks in the mid-frequency region have been identified in previous studies [14–17] and are summarized in a recent paper [9].

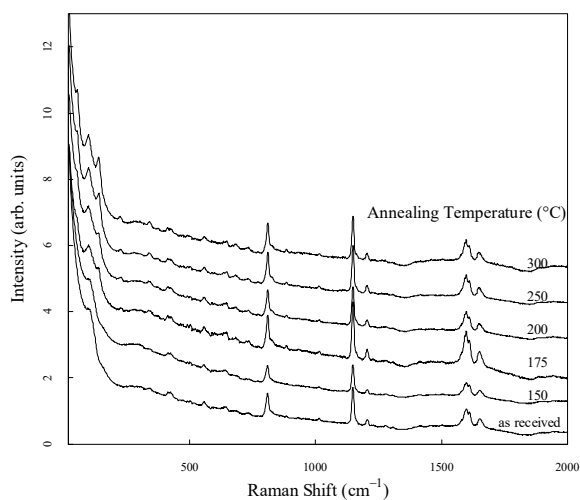


Figure 2. Raman spectra of PEEK with standardized in the range of 40 cm^{-1} to 2000 cm^{-1} .

To observe the spectral shape in more detail, the enlarged spectra of each region are shown in Fig. 3(a)–(d). Each spectrum was standardized in the area displayed on the horizontal axis. Figure 3(a) shows the peaks at 50 cm^{-1} , 97 cm^{-1} , 135 cm^{-1} in samples annealed at temperatures above $175\text{ }^{\circ}\text{C}$. In a previous study, we reported that the peak at 135 cm^{-1} was significantly related to crystallinity and is associated with intermolecular vibration modes. [19,28] The peak at 50 cm^{-1} was observed for the first time and was markedly dependent on the degree of crystallinity, similar to the peak at 135 cm^{-1} . It is clear that the peaks at 50 cm^{-1} and 135 cm^{-1} in the low-frequency region are very sensitive to crystallinity, although crystallinity dependence has been reported for the peaks, such as the peak center at 1644 cm^{-1} , intensity ratio of 1597 and 1607 cm^{-1} , intensity ratio of the bands at 800 and 810 cm^{-1} [14], and center frequency at 1146 cm^{-1} [32] and 1651 cm^{-1} [9] in the mid-frequency region. Furthermore, it is noteworthy that the peaks at 50 cm^{-1} and 135 cm^{-1} completely disappeared in the sample with 0% crystallinity.

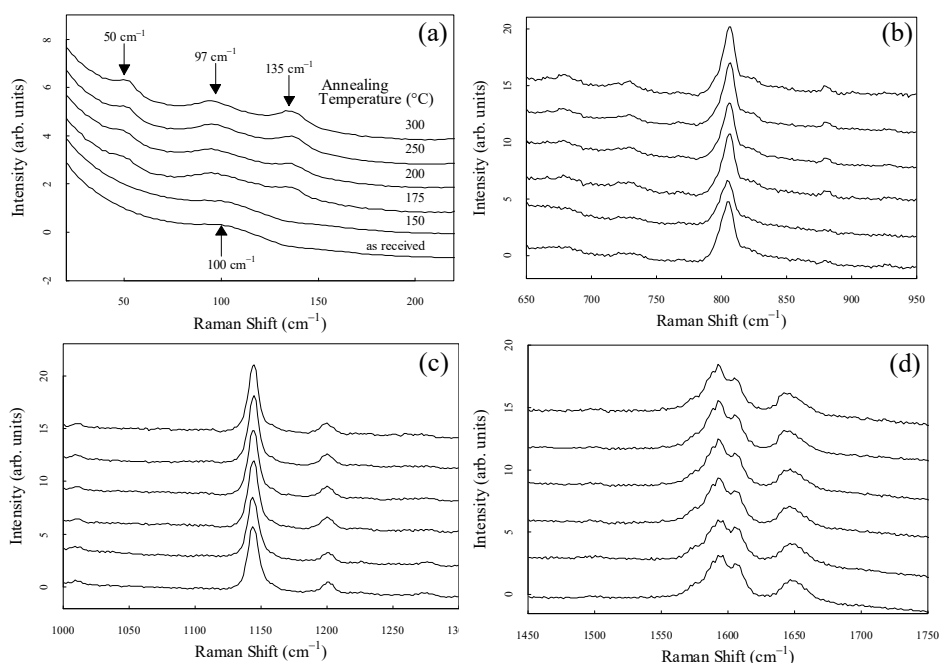


Figure 3. (a), (b), (c), and (d) show enlarged spectra at $20 - 220\text{ cm}^{-1}$, $650 - 950\text{ cm}^{-1}$, and $1000 - 1300\text{ cm}^{-1}$, and $1450 - 1750\text{ cm}^{-1}$, respectively. Each spectrum was standardized in the area displayed on the horizontal axis.

Raman spectra in the low-frequency region were decomposed into peaks expressed by a Lorentz function for the 50 cm^{-1} , 97 cm^{-1} and 135 cm^{-1} , a Gaussian function and a linear function for the baseline. The Lorentz function has intensity, half-width at half maximum, and center frequency as parameters. The Gaussian function representing the background with a center frequency of 0 cm^{-1} , and the half-width at half maximum and intensity were used as fitting parameters. All parameters were individually adjusted to attain the minimum chi-square value using Levenberg-Marquardt nonlinear least-squares optimization. An example of fitting the Raman spectra is shown in Fig. 4. The open circles show the experimental data, and the solid curves show the fitting results. The dashed lines represent decomposed elements.

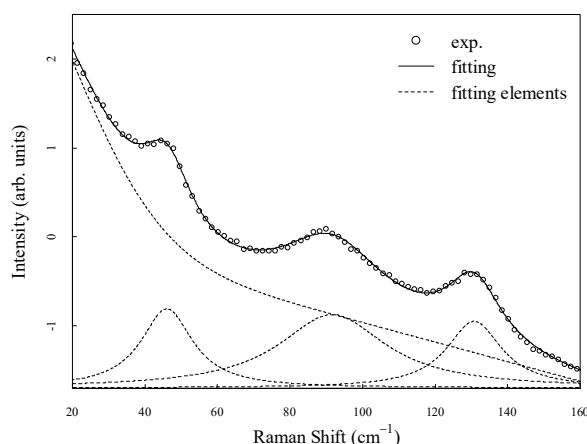


Figure 4. Typical example of fitting analysis of Raman spectra. The white circles represent the experimental data. The solid lines represent the fitted results. The dashed lines represent the decomposed elements (three peaks and baseline).

Figure 5 shows the intensity ratio between 50 cm^{-1} and 97 cm^{-1} ($I_{50\text{cm}^{-1}}/I_{97\text{cm}^{-1}}$) and the intensity ratio between 135 cm^{-1} and 97 cm^{-1} ($I_{135\text{cm}^{-1}}/I_{97\text{cm}^{-1}}$). The dashed line represents the eye-guide and is well-correlated. Both values increased as crystallinity increased. This result, including the peaks that disappeared in the amorphous state, suggests that the two peaks were influenced by intermolecular order through the same mechanism.

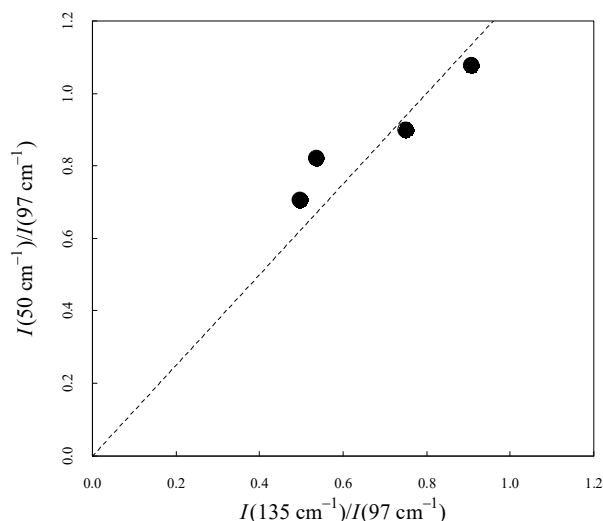


Figure 5. Correlation between $I_{50\text{cm}^{-1}}/I_{135\text{cm}^{-1}}$ and $I_{50\text{cm}^{-1}}/I_{97\text{cm}^{-1}}$. The dashed line represents the eye-guide.

3.2. DFT and MD Simulations

Simulations were performed to clarify the origin of the peak at 50 cm^{-1} . Figure 6 shows the Raman spectra calculated using DFT. Figure 6 (a), (b), and (c), which is modified Fig.3 in Ref[28], show the spectra of PEEK oligomers with different lengths, terminated with phenyl groups. The calculated molecular structures are shown on the right, where "Ph," "-O-," and "-CO-" represent the phenyl group (C_6H_5 - or $-\text{C}_6\text{H}_4$ -), ether, and ketone, respectively. Peaks (i)–(iii) in the gray shaded region are described in Ref. [28]. Figure 7 shows the atomic motion in the vibrational modes at approximately 50 cm^{-1} (peak (iv)) calculated for a single oligomer molecule using DFT. The peak at 50 cm^{-1} is roughly identified the motion of twisting of ketone and connected benzene rings (Ph-O-Ph), which is similar to the peak at 135 cm^{-1} (peak (ii)). The MD simulations were performed using LAMMPS. The video can be found in Supplemental Video S1 (the time interval corresponds to 50 cm^{-1}). The origins of the peaks at 50 cm^{-1} and 135 cm^{-1} were associated with Ph-CO-Ph-type intermolecular vibrational modes. In general, ketone groups have a high polarity. Therefore, it was

inferred that the ketone group plays a major role in the interactions between the molecules. The 50 cm^{-1} and 135 cm^{-1} modes are not observed in the amorphous state and are sensitive to crystallinity because these modes are related to ketone groups, which are strongly related to the intermolecular order.

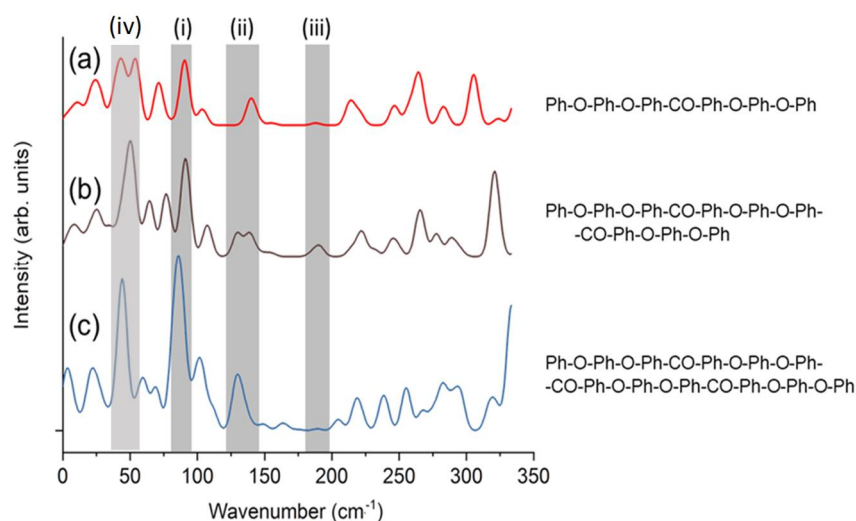


Figure 6. The DFT-calculated Raman spectra of phenyl-terminated PEEK oligomers are shown on the right. The peaks around $85\text{--}98\text{ cm}^{-1}$, $130\text{--}145\text{ cm}^{-1}$ and 190 cm^{-1} are labeled as (i), (ii), and (iii), respectively. (a–c) represent different lengths of a PEEK molecular chain; the structures of the molecules are shown in the right panel.

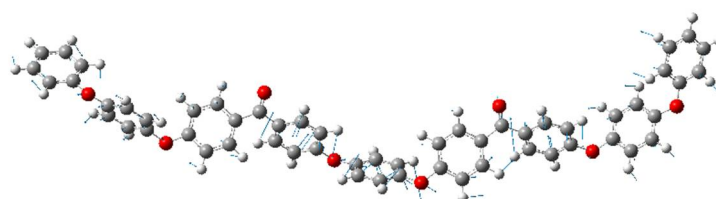
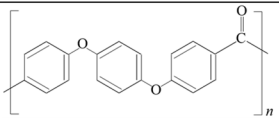
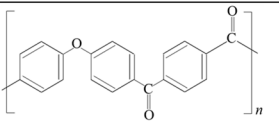


Figure 7. Atomic motion in the vibrational modes at 50 cm^{-1} calculated for a single oligomer molecule using DFT.

Delbé et al. observed three peaks at 77 cm^{-1} , 109 cm^{-1} , and 135 cm^{-1} in the low-frequency region of poly(ether ketone ketone) (PEKK)[31]. They considered that the peaks at 109 cm^{-1} and 135 cm^{-1} in PEKK corresponded to the peaks at 97 cm^{-1} and 135 cm^{-1} in PEEK, respectively, and discussed that the vibration frequency decreased because of the addition of a ketone group in PEKK. It seems plausible that the peak at 50 cm^{-1} in PEEK corresponds to the peak at 77 cm^{-1} in PEKK (Table 1). Among the three peaks in the low-frequency region observed for crystalline PEEK, two peaks assigned to ketone group vibrations disappeared in amorphous PEEK. In contrast, the peak assigned to the ketone group vibration was observed in even amorphous. It is presumed that the Ph-CO-Ph vibration mode is enhanced by intermolecular interactions in PEEK and by intramolecular interactions in PEKK. Our intention is to provide further clarification on this matter through extensive simulations that concentrate specifically on the ketone groups in the future.

Table 1. Raman peak in low-frequency region in PEEK and PEKK [31]. The insets represent the respective chemical formulae.

PEEK		PEKK		Assignment
crystal	amorphous	amorphous		
				
wavenumber (cm ⁻¹)		wavenumber (cm ⁻¹)		
50	Not observed	77		phonon Ph-CO-Ph
97	100	109		phonon Ph-O-Ph
135	Not observed	135		phonon Ph-CO-Ph

4. Conclusion

Low-frequency peaks in the Raman spectra of the amorphous PEEK were studied. An amorphous sample with zero crystallinity, as confirmed by WAXRD, was used in this study. The peaks at 50 cm⁻¹, which were observed for the first time, and 135 cm⁻¹ disappeared in the amorphous sample. The peak intensities at 135 cm⁻¹ and 50 cm⁻¹ increased as the crystallinity increased. This result, including the peaks that disappeared in the amorphous state, suggests that the two peaks were influenced by intermolecular order through the same mechanism. The peak at 50 cm⁻¹ indicates the twisting motion of the ketone and connected benzene rings (Ph-O-Ph), which is similar to the peak at 135 cm⁻¹ obtained using DFT and MD simulations. Furthermore, the peaks in the low-frequency region of PEEK and PEKK were considered, suggesting that the ketone group plays an important role.

Supplementary Materials: The following supporting information can be downloaded at the website of this paper posted on Preprints.org, Video S1: MD snapshots corresponding to vibration at 50 cm⁻¹. Available online: <https://youtu.be/sS23bM8gP8g> (accessed on 30 May 2024)

Author Contributions: Conceptualization, T. S., K. G., and M.Y.; experimental, T.N. and M. Y.; validation, M.Y.; supervision, N.I.; All the authors have read and agreed to the published version of the manuscript.

Funding: This work was supported by JSPS KAKENHI Grant Number 23H01310.

Institutional Review Board Statement: Not applicable.

Informed Consent Statement: Not applicable.

Data Availability Statement: Experimental data can be provided upon request.

Acknowledgments: This work was supported by JSPS KAKENHI Grant Number 23H01310.

Conflicts of Interest: The authors declare no conflict of interest.

References

- Biron, M., "Handbook of Thermoplastic Elastomers," William Andrew, 2012.
- Blundell, D. J.; Osborn, B. N., "The morphology of poly(aryl-ether-ether-ketone)" *Polymer*, **1983**, 24, pp. 953-958.
- Gao, S.-L.; Kim, J.-K., "Cooling rate influences in carbon fibre/PEEK composites. Part 1. Crystallinity and interface adhesion" *Composites Part A: Applied Science and Manufacturing*, **2000**, 31, pp. 517-530.
- Huo, P.; Cebe, P., "Temperature-dependent relaxation of the crystal-amorphous interphase in poly(ether ether ketone)" *Macromolecules*, **1992**, 25, pp. 902-909.
- Cogswell, F. N.; Hopprich, M., "Environmental resistance of carbon fibre-reinforced polyether etherketone" *Composites*, **1983**, 14, pp. 251-235.
- Comer, A. J.; Ray, D.; Obande, W. O.; Jones, D.; Lyons, J.; Rosca, I.; O' Higgins, R.M.; McCarthy, M.A., "Mechanical characterisation of carbon fibre-PEEK manufactured by laser-assisted automated-tape-placement and autoclave" *Composites Part A: Applied Science and Manufacturing*, **2015**, 69, pp. 10-20.
- Deignan, A.; Stanley, W.; McCarthy, M., "Insights into wide variations in carbon fibre/polyetheretherketone rheology data under automated tape placement processing conditions" *Journal of Composite Materials*, **2018**, 52, pp. 2213-2228.
- Regis, M.; Bellare, A.; Pascolini, T.; Bracco, P., "Characterization of thermally annealed PEEK and CFR-PEEK composites: Structure-properties relationships" *Polymer Degradation and Stability*, **2017**, 136, p. 121-130.

9. Doumeng, M. ; Makhlof, L. ; Berthet, F. ; Marsan, O. ; Delbé, K. ; Denape, J. ; Chabert, F., " A comparative study of the crystallinity of polyetheretherketone by using density, DSC, XRD, and Raman spectroscopy techniques" *Polymer Testing*, **2021**, 93, p. 106878,.
10. Bas, C. ; Battesti, P. ; Albérola, N. D., " Crystallization and melting behaviors of poly(aryletheretherketone) (PEEK) on origin of double melting peaks" *Journal of Applied Polymer Science*, **1994**, 53, p. 1745-1757,.
11. Uematsu, H. ; Kawasaki, T. ; Koizumi, K. ; Yamaguchi, A. ; Sugihara, S. ; Yamane, M. ; Kawabe, K. ; Ozaki, Y. ; Tanoue, S., " Relationship between crystalline structure of polyamide 6 within carbon fibers and their mechanical properties studied using Micro-Raman spectroscopy" *Polymer*, **2021**, 223, p. 123711.
12. Lee, Y. ; Porter, R. S., " Crystallization of poly(etheretherketone) (PEEK) in carbon fiber composites" *Polymer Engineering & Science*, **1986**, 26, p. 633-639.
13. Hsu, S. L. ; Patel, J. ; Zhao, W., "" Molecular Characterization of Polymers: A Fundamental Guide, **2021**, Chapter 10, p. 369.
14. Loudon, J. D., "Crystallinity in poly(aryl ether ketone) films studied by raman spectroscopy " *Polymer. Commun.*, **1986**, 27, p. 82-84,.
15. Everall, N. J. ; Chalmers, J. M. ; Ferwerda, R. ; van der Maas, J. H. ; Hendra, P. J., "Measurement of poly(aryl ether ether ketone) crystallinity in isotropic and uniaxial samples using Fourier transform-Raman spectroscopy: A comparison of univariate and partial least-squares calibrations" *Journal of Raman Spectroscopy*, **1994**, 25, p. 43-51,.
16. Briscoe, B. J. ; Stuart, B. H. ; Thomas, P. S. ; Williams, D. R., "A comparison of thermal- and solvent-induced relaxation of poly(ether ether ketone) using Fourier transform Raman spectroscopy" *Spectrochimica Acta Part A: Molecular and Biomolecular Spectroscopy*, **1991**, 47, p. 1299-1303,.
17. Ellis, G. ; Naffakh, M. ; Marco, C. ; Hendra, P. J., " Fourier transform Raman spectroscopy in the study of technological polymers Part 1: poly(aryl ether ketones), their composites and blends " *Spectrochimica Acta Part A: Molecular and Biomolecular Spectroscopy*, **1997**, 53, p. 2279-2294.
18. Qian, X. ; Wang, X. ; Zhong, J. ; Zhi, J. ; Heng, F. ; Zhang, Y. ; Song, S., " Effect of fiber microstructure studied by Raman spectroscopy upon the mechanical properties of carbon fibers" *Journal of Raman Spectroscopy*, **2019**, 50, p. 665-673,.
19. Yamaguchi, M. ; Kobayasi, S. ; Numata, T. ; Kamihara, N. ; Shimada, T. ; Jikei, M. ; Muraoka, M., " Evaluation of crystallinity in carbon fiber-reinforced poly(ether ether ketone) by using infrared low frequency Raman spectroscopy" *Journal of Applied Polymer Science*, **2022**, 139, p. 51677,.
20. Walker, G. ; Römann, P. ; Poller, B. ; Löbmann, K. ; Grohganz, H. ; Rooney, J. S. ; Huff, G. S. ; Smith, G. P. S. ; Rades, T. ; Gordon, K. C. ; Strachan, C. J. ; Fraser-Miller, S. J., " Probing Pharmaceutical Mixtures during Milling: The Potency of Low-Frequency Raman Spectroscopy in Identifying Disorder" *Molecular Pharmaceutics*, **2017**, 14, p. 4675-4684
21. Lipiäinen, T. ; Fraser-Miller, S. J. ; Gordon, K. C. ; Strachan, C. J., "Direct comparison of low- and mid-frequency Raman spectroscopy for quantitative solid-state pharmaceutical analysis" *Journal of Pharmaceutical and Biomedical Analysis*, **2018**, 149, p. 343-350,.
22. Yamamoto, S. ; Ohnishi, E. ; Sato, H. ; Hoshina, H. ; Ushikawa, D. ; Ozaki, Y., " Low-Frequency Vibrational Modes of Nylon 6 Studied by Using Infrared and Raman Spectroscopies and Density Functional Theory Calculations" *Journal of Physical Chemistry B*, **2019**, 123, p. 5368-5376.
23. Yamamoto, S. ; Miyada, M. ; Sato, H. ; Hoshina, H. ; Ozaki, Y., " Low-Frequency Vibrational Modes of Poly(glycolic acid) and Thermal Expansion of Crystal Lattice Assigned On the Basis of DFT-Spectral Simulation Aided with a Fragment Method" *Journal of Physical Chemistry B*, **2017**, 121, p. 1128-1138.
24. Funaki, C. ; Yamamoto, S. ; Hoshina, H. ; Ozaki, Y. ; Sato, H., " Three different kinds of weak C-H \cdots O=C inter- and intramolecular interactions in poly(ϵ -caprolactone) studied by using terahertz spectroscopy, infrared spectroscopy and quantum chemical calculations" *Polymer*, **2018**, 137, p. 245-254.
25. Funaki, C. ; Toyouchi, T. ; Hoshina, H. ; Ozaki, Y. ; Sato, H., "Terahertz Imaging of the Distribution of Crystallinity and Crystalline Orientation in a Poly(ϵ -caprolactone) Film" *Applied Spectroscopy*, **2017**, 71, p. 1537-1542,.
26. Kaneko, T. ; Hirai, N. ; Ohki, Y., " Terahertz absorption spectroscopy of poly(ether ether ketone) " *Proceedings of 2017 International Symposium on Electrical Insulating Materials*, **2017**, p. 539-542.
27. Hiroshiba, N. ; Akiraka, M. ; Kojima, H. ; Ohnishi, S. ; Ebata, A. ; Tsuji, H. ; Tanaka, S. ; Koike, K. ; Ariyoshi, S., " Broadband infrared absorption spectroscopy of low-frequency inter-molecular vibrations in crystalline poly(L-lactide)" *Physica B: Condensed Matter*, **2023**, 649, p. 414488,.
28. Yang, X. ; Yokokura, S. ; Nagahama, T. ; Yamaguchi, M. ; Shimada, T., " Molecular Dynamics Simulation of Poly(Ether Ether Ketone)(PEEK) Polymer to Analyze Intermolecular Ordering by Low Wavenumber Raman Spectroscopy and X-ray Diffraction" *Polymers*, **2022**, 14, p. 5406,.
29. Dawson, P. C. ; Blundell, D.J., *Polymer Communications*, **1980**, 21, 5, p. 577-578,.
30. Li, Q. ; Perrie, W. ; Tang, Y. ; Allegre, O. ; Ho, J. ; Chalker, P. ; Li, Z. ; Edwardson, S. ; Dearden, G., " A study on ultrafast laser micromachining and optical properties of amorphous polyether(ether)ketone (PEEK) films " *Procedia CIRP*, **2020**, 94, p. 840-845,.

31. Delbé, K. ; Chabert, F., " Raman Spectroscopy Investigation on Amorphous Polyetherketoneketone (PEKK) " *Vibrational Spectroscopy*, 2023, 129, p. 103620.
32. Doumeng, M. ; Ferry, F. ; Delbé, K. ; Mérian, T. ; Chabert, F. ; Berthet, F. ; Marsan, O. ; Nassiet, V. ; Denape, J., " Evolution of crystallinity of PEEK and glass-fibre reinforced PEEK under tribological conditions using Raman spectroscopy " *Wear*, 2019, 426–427, Part B, p. 1040-1046

Disclaimer/Publisher's Note: The statements, opinions and data contained in all publications are solely those of the individual author(s) and contributor(s) and not of MDPI and/or the editor(s). MDPI and/or the editor(s) disclaim responsibility for any injury to people or property resulting from any ideas, methods, instructions or products referred to in the content.